

Structural Characterization of Lateral-grown 6H-SiC a/m-plane Seed Crystals by Hot Wall CVD Epitaxy

Ouloide Yannick Goue¹, Balaji Raghothamachar¹, Michael Dudley¹, Andrew J. Trunek², Philip G. Neudeck², Andrew A. Woodworth², David J. Spry²

¹Department of Materials Science and Engineering Stony Brook University, Stony Brook, NY 11794-2275, USA

²NASA Glenn Research Center, 21000 Brookpark Road, MS 77-1, Cleveland, OH 44135 USA

ABSTRACT

The performance of commercially available silicon carbide (SiC) power devices is limited due to inherently high density of screw dislocations (SD), which are necessary for maintaining polytype during boule growth and commercially viable growth rates. The NASA Glenn Research Center (GRC) has recently proposed a new bulk growth process based on axial fiber growth (parallel to the c-axis) followed by lateral expansion (perpendicular to the c-axis) for producing multi-faceted m-plane SiC boules that can potentially produce wafers with as few as one SD per wafer. In order to implement this novel growth technique, the lateral homoepitaxial growth expansion of a SiC fiber without introducing a significant number of additional defects is critical. Lateral expansion is being investigated by hot wall chemical vapor deposition (HWCVD) growth of 6H-SiC a/m-plane seed crystals (0.8mm x 0.5mm x 15mm) designed to replicate axially grown SiC single crystal fibers. The post-growth crystals exhibit hexagonal morphology with approximately 1500 μm (1.5 mm) of total lateral expansion. Preliminary analysis by synchrotron white beam x-ray topography (SWBXT) confirms that the growth was homoepitaxial, matching the polytype of the respective underlying region of the seed crystal. Axial and transverse sections from the as-grown crystal samples were characterized in detail by a combination of SWBXT, transmission electron microscopy (TEM) and Raman spectroscopy to map defect types and distribution. X-ray diffraction analysis indicates the seed crystal contained stacking disorders and this appears to have been reproduced in the lateral growth sections. Analysis of the relative intensity for folded transverse acoustic (FTA) and optical (FTO) modes on the Raman spectra indicate the existence of stacking faults. Further, the density of stacking faults is higher in the seed than in the grown crystal. Bundles of dislocations are observed propagating from the seed in m-axis lateral directions. Contrast extinction analysis of these dislocation lines reveals they are edge type basal plane dislocations that track the growth direction. Polytype phase transition and stacking faults were observed by high-resolution TEM (HRTEM), in agreement with SWBXT and Raman scattering.

INTRODUCTION

Silicon carbide (SiC) is a wide-band gap compound semiconductor that possesses excellent electronic, thermal and mechanical properties, which make it suitable for a variety of applications [1-3] such as high-power switching devices, light emitting diodes (LEDs) and junction field effect transistors (JFETs) [4-6]. The presence of high density of screw dislocations,

polytype inclusions and other defects limit the performance of these devices [4-6]. Commercial SiC single crystals are grown by the physical vapor transport (PVT) method [6]. One of the main challenges of growing SiC is polytype control. The factors affecting the nature of the grown polytype have been studied [6-9]. Screw dislocations have been reported to act as step sources that help maintain polytypes and commercially viable growth rates [10].

Attempts at growing single crystals with low density of screw dislocations (SD), such as the PVT repeated a-face (RAF) growth process, [9, 11] are involved and the crystals grown contained a relatively high dislocation density and stacking fault (SF) [9]. Researchers at NASA Glenn Research Center (GRC) have recently proposed a new bulk growth process based on axial fiber growth (parallel to the c-axis) followed by lateral (perpendicular to the c-axis) expansion by hot wall chemical vapor deposition (HWCVD), producing SiC boules. The resulting boules will potentially produce wafers with as few as one SD per wafer [12]. In order to implement this novel growth technique, the lateral homoepitaxial growth expansion of a SiC fiber without introducing a significant number of additional defects is critical.

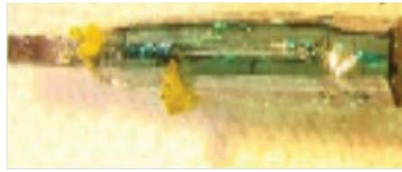
In this paper, we have carried out detailed characterization on the HWCVD-grown lateral enlargement of 6H-SiC a/m-plane seed crystals designed to replicate axially grown SiC single crystal fibers. As-grown crystals were analyzed by SEM and synchrotron white beam X-ray topography (SWBXT) followed by detailed analysis of axial and transverse sections from the as-grown crystals by a combination of SWBXT, HRTEM and Raman scattering to map defect types and distribution.

EXPERIMENT

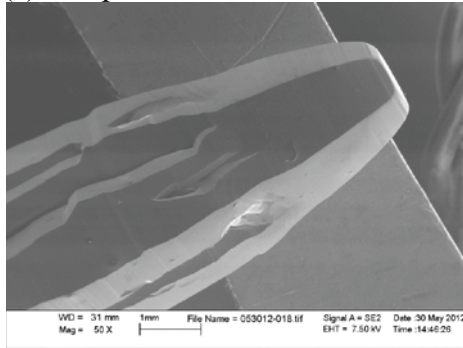
4H/6H-SiC seed crystals (0.8 mm x 0.5 mm x 15 mm) with two m-plane faces and two a-plane faces were subjected to lateral growth by HWCVD between 8 -16 hours of growth over multiple growth runs at NASA GRC [13]. The as-grown crystals have evolved towards the hexagonal crystal symmetry (Fig. 1(a)) of the SiC crystal structure with the greatest lateral expansion in the $\langle 1\bar{1}00 \rangle$ directions. SEM (Fig. 1(b)) and SWBXT (Fig. 1(c)) studies were carried out on the as-grown crystals to map the morphology and evaluate the general crystalline quality. The crystals were then sectioned into axial (m (1-100) and a-(11-20) plane) and transverse (c-plane (0001)) slices and mechanically polished with diamond abrasive films. The samples were then investigated using a combination of SWBXT, TEM and Raman scattering. Overall defect microstructures of the m/a-plane and c-plane samples were imaged using SWBXT in transmission geometry at the Stony Brook topography station, Beamline X19C, National Synchrotron Light Source (NSLS), Brookhaven National Laboratory (BNL). The images were recorded on Agfa Structurix D3-SC films. From the analysis of the recorded topographs, regions were selected for further characterization. First, Raman scattering was measured for a region across the seed crystal. This enabled determination of the inhomogeneity of the seed crystal. Then TEM specimens were prepared parallel to the [11-20] direction of both axial and transverse samples. They were cut at the interface across the seed and the grown crystal. HRTEM experiments were conducted on a JEOL 2100F at the Center for Functional Nanomaterials (CFN) at BNL with an accelerating voltage of 200keV.



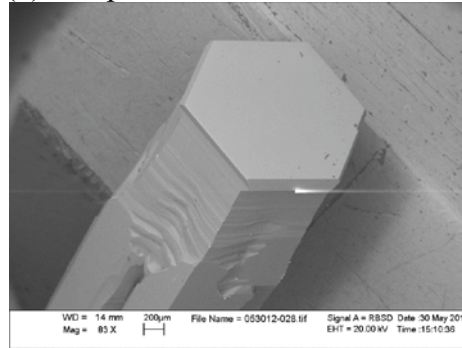
(a) Sample 1



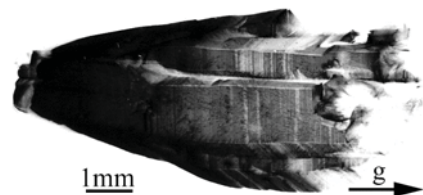
(b) Sample 2



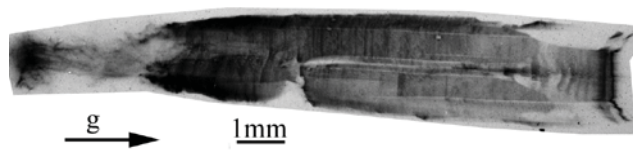
(c) Sample 1



(d) Sample 2



(e) Sample 1



(f) Sample 2

Figure 1. As-grown laterally expanded 4H/6H-SiC crystals(a-b) Optical photographs (yellow crystallites are of 3C-SiC polytype) and (c-d) SEM micrographs showing the hexagonal morphology; (e-f) Reflection X-ray topographs showing the strain-free as-grown surfaces of the single crystals.

RESULTS AND DISCUSSION

SWBXT topographs of the as-grown crystals (Fig. 1(c)) reveal the hexagonal morphology and a strain-free surface characterized primarily by steps as observed in SEM micrographs. X-ray diffraction pattern analysis reveals that while the seed crystal contained both 4H and 6H polytypes, the lateral grown material is only of 6H type, the 4H portion of the crystal was mounted in the graphite carrier and not subjected to growth reactants. In order to study the detailed defect distribution, axial and transverse slices were cut from the crystals. Figure 2 shows the X-ray topographs from the axial-cut sample. Other than the polishing marks and surface artifacts, the samples are characterized by linear defects propagating from the seed in the middle and running parallel to the basal planes. These are likely basal plane dislocations, but stacking faults can also be expected to be present, which has been reported [14]. Examination of one of the transverse c-plane slices revealed a central seed region (Fig. 3) characterized by high defect densities from which bundles of dislocations emanate along the m-axis directions. These dislocations appear to be mostly replicated from the seed although nucleation of new dislocations at the seed-epilayer interface cannot be ascertained due to the high dislocation densities involved. Any stacking disorders present in the seed will also likely be replicated into the epilayer, albeit at a possibly lower density. Analysis of these dislocation bundles by $g \cdot b = 0$ and $g \cdot b \times l = 0$ criteria

(where \mathbf{g} is the reflection vector and \mathbf{b} is the Burgers vector) reveals these are edge-type $1/3\langle 11-20 \rangle$ dislocations.

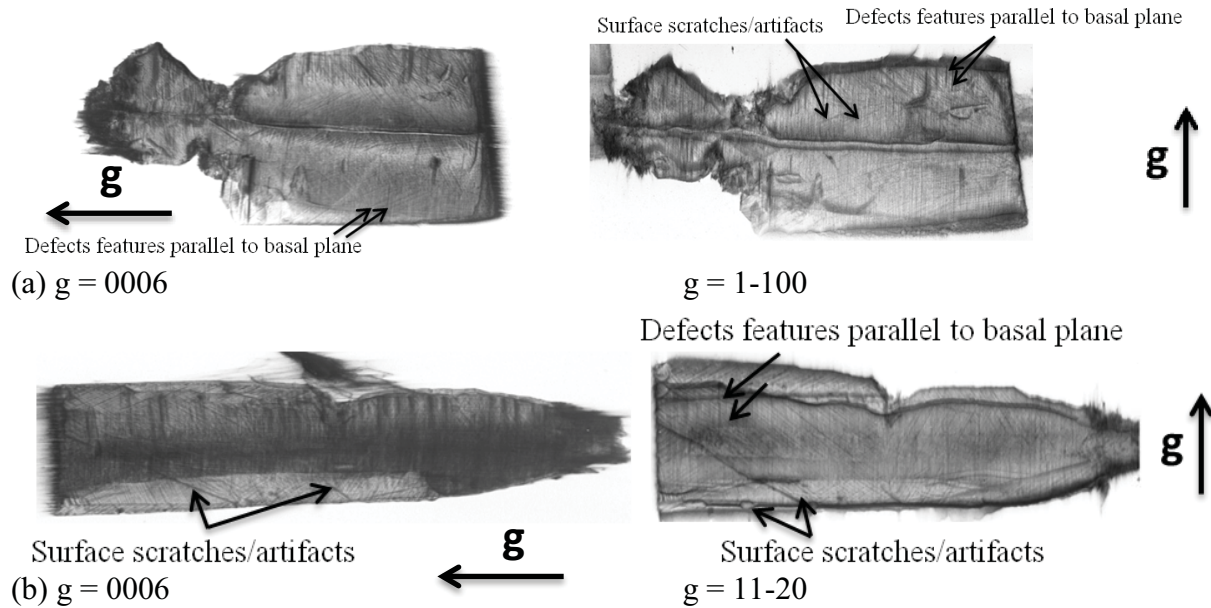


Figure 2. Transmission X-ray topographs of (a) a-plane cut (from Sample 1) (b) m-plane axial-cut (from Sample 2) as-grown crystal samples.

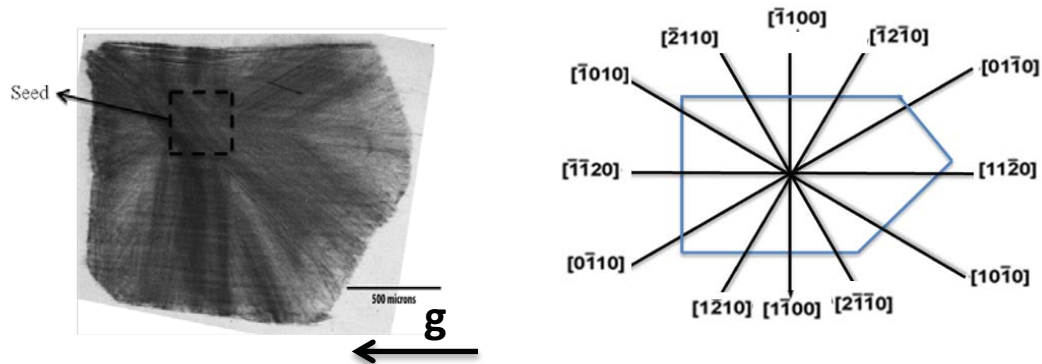


Figure 3. Transmission X-ray topograph of transverse (0001) slice as-grown crystal sample along with a sketch showing the crystallographic directions. Note the bundles of dislocations running along the $\langle 1-100 \rangle$ directions.

Since the dislocation bands emanate from the seed region of the crystal, a map of the seed crystal region along with the corresponding spectra was obtained by Raman scattering. This allowed the determination of the inhomogeneity of the seed and confirmed the presence of stacking disorders originating from the seed. Raman spectra and corresponding mapping are shown in Fig. 4. Raman intensity profile and frequency shift of SiC polytypes have well been documented [15, 16]. Furthermore, studies have been carried out, which harness the nondestructive character of Raman scattering to study polytypism and stacking disorder in SiC [15, 16]. Analysis of the relative intensity for folded transverse acoustic (FTA) and optical (FTO) modes on the Raman spectra indicate a high stacking disorder in the seed region.

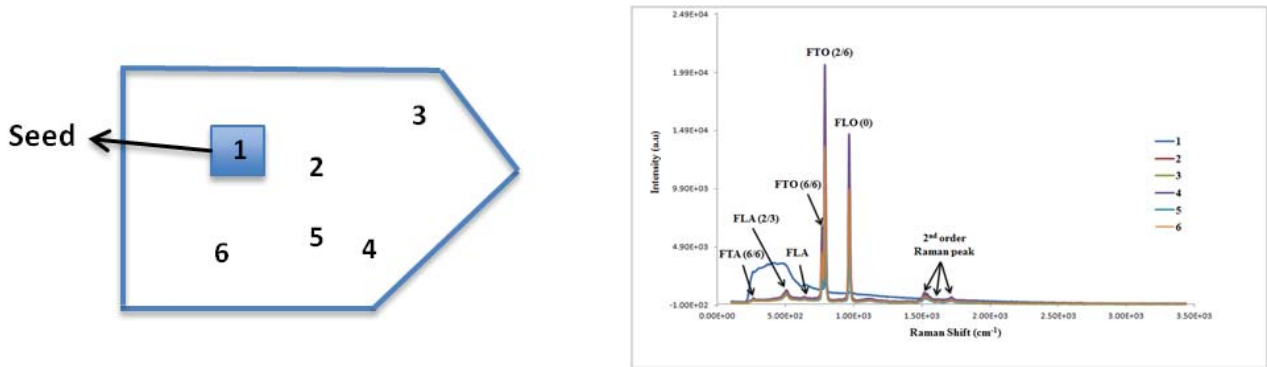


Figure 4. Raman mapping of a transverse slice (a) and corresponding Raman spectra (b)

Based on the results of the Raman mapping, TEM specimens were prepared by focused ion beam (FIB) parallel to the [11-20] direction for both axial and transverse samples. High-resolution TEM (HRTEM) images of the TEM specimen for the transverse sample reveal the existence of 3C and 8H-SiC polytypes (Fig. 5). These polytypes could be replicated from the seed or formed during growth. Possible polytype transformation mechanisms have been extensively studied [17] and currently additional HRTEM studies are being carried out to deduce the mechanism of transformation in these laterally expanded crystals.

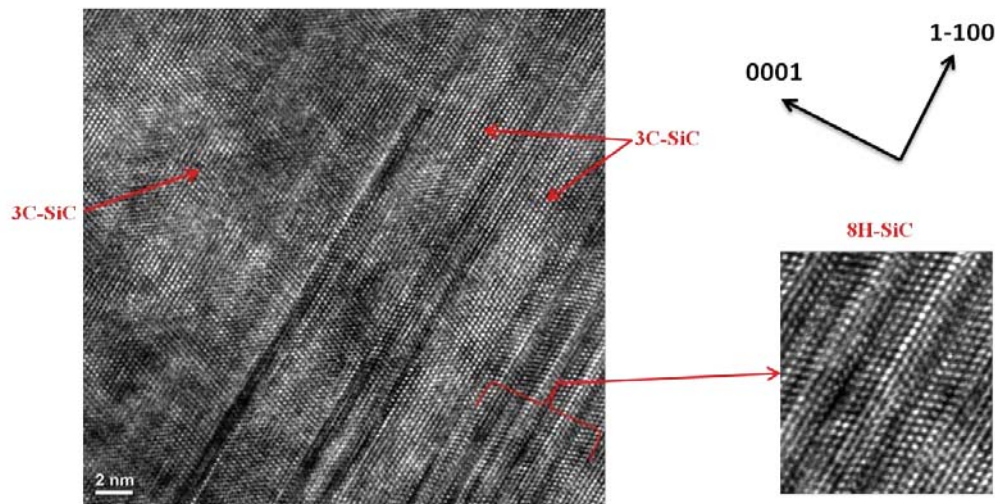


Figure 5. HRTEM image for 6H-SiC axial slice sample showing 3C and 8H-SiC polytypes.

CONCLUSIONS

Structural characterization of lateral-grown 6H-SiC a/m-plane seed crystals grown by HWCVD were carried out using a combination of SWBXT, Raman scattering and HRTEM. Defect types and distribution were identified. Lateral expanded material is single crystal but contains bundles of edge basal plane dislocations propagating from the seed/seed-epilayer interface and stacking disorders most of which are also replicated from the seed.

ACKNOWLEDGMENTS

Work supported by NASA Glenn Research Center and the US Department of Energy (DOE) Vehicle Technology Program via Space Act Agreement (SAA3-1048) (DOE IA # DE-EE0001093/ 001) monitored by Susan Rogers (DOE). NASA Postdoctoral Program Fellowship supported by NASA Vehicle Systems Safety Technologies Project in the Aviation Safety Program. SWBXT work was carried out at Stony Brook Topography Facility (Beamline X19C) at the NSLS, Brookhaven National Laboratory, which is supported by the U.S. DOE. under Grant No. DE-AC02-76CH00016. HRTEM work carried out at the Center for Functional Nanomaterials, Brookhaven National Laboratory, which is supported by the U.S. DOE, Office of Basic Energy Sciences, under Contract No. DE-AC02-98CH10886. Raman scattering performed by Nicholas Heller.

REFERENCES

- [1] J.B. Casady and R. W. Johnson, *Solid-State Electron.* 39, 1409 (1996).
- [2] Pasqualina M. Sarro, *Sens. Actuators A* 82, 210 (2000).
- [3] J.W. Palmour, J.A. Edmond, H.S Kong and C.H Carter Jr., *Physica B: Condens. Matter* 185, 461 (1993).
- [4] A. Grekov, Q. Zhang, H. Fatima, A. Agarwal and T.S Sudarshan, *Microelectron. Reliab.* 48, 1664 (2008).
- [5] H. Fujiwara, T. Kimoto, T. Tojo and G. Matsunami, *Appl. Phys. Lett* 87, 51912 (2005).
- [6] K. Semmelroth, N. Schulze and G. Pensl, *J. Phys.: Condens. Matter* 16, 1597 (2004)
- [7] S. Harada, K. Seki, Y. Yamamoto, C. Zhu, S. Arai, J. Yamsaki, N. Tanak and T. Ujihara, *Cryst. Growth Des.* 12, 3209 (2012).
- [8] C. Liu, X. Chen, T. Peng, B. Wang, W. Wang and G. Wang, *J. Cryst. Growth* 394, 126 (2014).
- [9] Daisuke Nakamura, *Mater. Sci. Forum* 527-529, 3 (2005).
- [10] J. Li, O. Filip, B.M Epelbaum, X. Xu, M. Bickermann and A. Winnacker, *J. Cryst. Growth* 308, 41 (2007).
- [11] J. A. Powell, P. G. Neudeck, A. J. Trunek and D. J. Spry, U.S patent No. 7,449,065 (11 November 2008).
- [12] A.J. Trunek, P.G Neudeck, A.A Woodworth, J.A Powell, D.J Spry, B. Raghothamachar and M. Dudley, *Mater. Sci. Forum* 717-720, 33 (2012).
- [13] H.J. Rost, M. Schmidbauer, D. Siche and R. Fornari, *J. Cryst. Growth* 290, 137 (2006).
- [14] T. Mitani, S. Nakashima, H. Okumura and H. Nagasawa, *Mater. Sci. Forum* 527-529, 343 (2005).
- [15] S. Rohmfeld, M. Hundhausen, and L. Ley, *Phys. Rev. B* 58, 9858 (1998).
- [16] W. K. Burton, N. Cabrera, F. C. Frank, *Philos. Trans. R. Soc. London*, 243A, 299 (1951).
- [17] P. Pirouz and J.W. Yang, *Ultramicroscopy* 51, 189 (1993).